tunneling conductance, $\Delta\sigma/\sigma$, measured by inelastic tunneling spectroscopy. We have $\Delta\sigma/\sigma \sim 0.015$ for both CO/Cu (*14*) and CO/Pd(110), so that the hopping probability per tunneling electron should be $10^{-11}$, which is of the same order of magnitude as the experimental results. From the first-order process, we also estimate a similar contribution to the hopping probability. The situation is markedly different for CO/Cu(110): the magnitude of $\delta\omega$ is much smaller, and $n$ and $n_0$ are much greater than for CO/Pd(110). These differences make the transition much more difficult. For CO/Cu (110), we estimate $P \approx 10^{-26}$ for the second-order process and $P \approx 10^{-53}$ for the first-order process.

The results for tunneling-induced lateral motion of adsorbates presented above should open ways for further investigation. We show an example in Fig. 4 where lateral motion is induced on a CO molecule at the edge of an 1D array on Pd(110) at 4.8 K. The array is formed by dosing a submonolayer of CO at room temperature before the sample is cooled to 4.8 K. In this process, the CO molecules spontaneously form an ordered structure that has two times the periodicity of the substrate along the $[1\bar{1}0]$ direction (*23*) (Fig. 4A). We applied the 1D dose-and-scan method on the array of seven molecules at the arrow of Fig. 4A. With the dosing of electrons at mark "a" and "c" in Fig. 4B, a group of CO molecules are shifted simultaneously to the right, leaving the target molecule at its original position. The ability to shift an array of adsorbates is one of the fundamental requirements for the proposed atom relay devices (*24*). More generally, we believe that the manipulation of adsorbates by inducing their lateral hopping through dosing of tunneling electrons, may be a useful tool in nanotechnology and for basic research in surface dynamics.

### References and Notes

1. G. Fedorus *et al.*, *Surf. Sci.* **251–252**, 846 (1991).
2. H. J. Jansch, J. Xu, J. T. Yates Jr., *J. Chem. Phys.* **99**, 721 (1993).
3. P. Avouris, *Acc. Chem. Res.* **18**, 95 (1995).
4. T. C. Shen *et al.*, *Science* **268**, 1590 (1995).
5. B. C. Stipe *et al.*, *Phys. Rev. Lett.* **78**, 4410 (1997).
6. B. C. Stipe, M. A. Rezaei, W. Ho, *Science* **279**, 1907 (1998).
7. ———, *Phys. Rev. Lett.* **81**, 1263 (1998).
8. The STM images reported here were taken at 4.8 K with a commercial STM (Omicron LT) in ultrahigh vacuum. The Pd(110) and Cu(110) were cleaned with a standard procedure described previously. The molecules of CO are dosed on the surface through a dosing tube located near the sample surface.
9. H. Kato, H. Okuyama, S. Ichihara, M. Kawai, J. Yoshinobu, *J. Chem. Phys.* **112**, 1925 (2000).
10. R. Raval, S. Haq, M. A. Harrison, G. Blyholder, D. A. King, *Chem. Phys. Lett.* **167**, 391 (1990).
11. N. Kitamura, M. G. Lagally, M. B. Webb, *Phys. Rev. Lett.* **71**, 2082 (1993).
12. The dosing event was executed with fixed tunneling current (7 nA) and the dosing period (1 s) for all applied voltages. The hopping probability was defined as the number of events in which the change of the bonding site occurs out of the total number of dosing events. We do not know exactly when the hopping occurs in the dosing period of 1 s. Thus, the remaining time after the event is a dead-time that makes the probability smaller. However, since the probability per event was chosen to be <0.1, the error is <5% of the value shown in the figure.
13. H. Kato, M. Kawai, J. Yoshinobu, *Phys. Rev. Lett.* **82**, 1899 (1999).
14. L. J. Lauhon, W. Ho, *Phys. Rev. B* **60**, R8525 (1999).
15. Again, the error bar of 5% should be considered as due to the dead-time effect.
16. B. G. Briner, M. Doering, H. P. Rust, A. M. Bradshaw, *Science* **278**, 257 (1997).
17. For details, see B. N. J. Persson, H. Ueba, *Surf. Sci.*, in press.
18. E. Schweizer *et al.*, *Surf. Sci.* **213**, 49 (1989).
19. T. A. Germer, J. C. Stephenson, E. J. Heilweil, R. R. Cavanagh, *J. Chem. Phys.* **101**, 1704 (1994).
20. M. Trenary, K. J. Uram, F. Bozso, J. T. Yates Jr., *Surf. Sci.* **146**, 269 (1984).
21. B. N. J. Persson, R. Ryberg, *Phys. Rev. Lett.* **54**, 2119 (1985).
22. J. Ellis, J. P. Toennies, G. Witte, *J. Chem. Phys.* **102**, 5059 (1995).
23. T. Komeda, Y. Kim, M. Kawai, *Jpn. J. Appl. Phys. Part 1* **40**, 4403 (2001).
24. Y. Wada, T. Uda, M. Lutwyche, S. Kondo, S. Heike, *J. Appl. Phys.* **74**, 7321 (1993).
25. Financial support was provided (in part) by the Grant-in-Aid for Scientific Research on Priority Areas "Surface Chemistry of Condensed Molecules" from the Japanese Ministry of Education, Culture, Sports, Science and Technology.

14 December 2001; accepted 12 February 2002

# Laser-Induced Selectivity for Dimerization Versus Polymerization of Butadiene Under Pressure

**Margherita Citroni,[1] Matteo Ceppatelli,[1] Roberto Bini,[1,2]* Vincenzo Schettino[1,2]**

**The pressure-induced chemical reaction of liquid butadiene was studied by Fourier transform infrared spectroscopy in a diamond anvil cell. Dimerization was found to occur above 0.7 gigapascal, giving vinylcyclohexene according to a cyclo-addiction reaction and only a trace amount of polybutadiene forms. By irradiating the high-pressure sample with a few milliwatts of the 488-nanometer argon$^+$ laser line, the dimerization was completely inhibited, and the rapid formation of pure *trans*-polybutadiene was observed. The use of different excitation wavelength allows us to emphasize the selectivity of the process and to identify the active role of the $2^1A_g$ state in this pressure- and laser-induced chemical reaction.**

The outcomes of chemical reactions depend not only on energetics but on how molecules are oriented before reaction. In solution, steric effects can be used to favor particular orientations of reactants to guide reactivity and stereochemistry, and surface effects, whether exerted by heterogeneous catalysts or enzyme pockets, can also favor particular orientations of reactants. In the solid-state reactions, crystal lattices offer an even greater degree of geometrical constraint of reactants, but there are few examples of controlling reaction conditions (such as temperature and pressure) to select different reaction pathways. Chemical transformations occurring in molecular crystals at high pressure have been reported in a few cases (*1–9*) . Recently, we have also shown that at high pressure, laser irradiation and photochemical effects are a further effective regulatory tool of the reaction mechanism with the twofold effect of changing the pure pressure-induced reaction pathway and lowering the reaction pressure (*5*, *8*). This makes high-pressure reactions an appealing preparation method for large-volume applications. Here, we used geometrical constraints to induce selective chemical reactivity by applying ultrahigh pressures with a diamond anvil cell (DAC), thus varying the relative distances and orientations between molecules, and selective laser irradiation to control excitation. By simply balancing these two parameters, we were able to induce and fully control the quantitative transformation of liquid butadiene to a simple dimer (vinylcyclohexene) or to a highly stereoregular polymer (*trans*-polybutadiene).

We were interested in studying *trans*-butadiene, an unsaturated very reactive molecule, because it can give rise to a variety of reaction products. Butadiene is also extremely unstable at ambient conditions, dimerization being the main reaction pathway (*10*). The dimerization is a second-order cyclo-addition reaction. Three

---

[1] Dipartimento di Chimica dell'Università di Firenze, Polo Scientifico, Via della Lastruccia 3, I-50019 Sesto Fiorentino, Firenze, Italy. [2] LENS, European Laboratory for Non-linear Spectroscopy and INFM, Polo Scientifico, Via Carrara 1, I-50019 Sesto Fiorentino, Firenze, Italy.

*To whom correspondence should be addressed. E-mail: bini@srv.chim.unifi.it

different dimers can be obtained depending on the mechanism (Scheme 1): (i) $[2\pi + 2\pi]$ cyclo-addition yielding 1,2-divinylcyclobutane; (ii) $[4\pi + 4\pi]$ cyclo-addition, giving 1,5-cyclooctadiene; and (iii) $[4\pi + 2\pi]$, the Diels-Alder reaction, giving 4-vinylcyclohexene, which is the main reaction product. Polymerization occurs only in the liquid phase or in solution at high temperature and only if catalysts and radical initiators are used (*11*). Under these conditions, polybutadiene is obtained as the mixture of the trans and cis isomers found in commercial polybutadiene.

In the present experiment (*12*), after loading the cell with liquid butadiene, the pressure was increased in steps of 0.2 to 0.3 kbar, and the infrared (IR) spectrum was monitored for more than 10 hours at each pressure. At ~0.7 GPa, new IR bands slowly grew with time superimposed on those of liquid butadiene. The reaction was followed for several days up to the complete transformation of the monomer in a recoverable product that essentially consists of pure vinylcyclohexene (Fig. 1A). The region between 600 and 1200 cm$^{-1}$ was selected because in this frequency range the absorptions due to the vinylcyclohexene and to the polymer are easily distinguished. The strongest band of polybutadiene occurs at 973 cm$^{-1}$, between the two bands of the monomer at 913 and 1016 cm$^{-1}$, and for vinylcyclohexene characteristic bands occur at 659, 671, and 731 cm$^{-1}$. The purely pressure-induced transformation mainly produces the dimer, with only trace amounts of the polymer. If the pressure was raised up to about 1 GPa, the dimerization rate increased considerably, but there was no appreciable effect on the polymerization process. Below 280 K, the liquid does not react on compression but freezes, giving a disordered solid. The reaction in the solid phase is currently under investigation.

In the pressure-induced polymerization of solid acetylene, an important role is played by laser irradiation (*5*). To investigate whether this effect is also important in the present case, we irradiated the sample with the 488- or 458-nm lines of an Ar$^+$ laser after the pressure was increased to 0.6 to 0.8 GPa. A few irradiation cycles (two or three) with a duration of 2 hours and with a typical power ranging between 10 and 20 mW were sufficient to induce the polymerization reaction and inhibit dimerization. As can be seen in Fig. 1B, the intensity of the bands assigned to the polymer rapidly increased and the formation of vinylcyclohexene was inhibited. Visual inspection of the sample revealed the formation of a transparent solid product in the cell. The polymer bands did not intensify with irradiation at 514.5 nm (Ar$^+$ line), thus revealing an energy threshold for the photochemical process. The IR spectrum of the recovered solid compound is identical to the spectrum of the commercial polymer (Aldrich: 36% cis, 59% trans, and 5% 1,2 adduct) except for the absence of the bands characteristic of the cis polymer (Fig. 2) (*13*). The selectivity of the photo-assisted high-pressure reaction to give a trans-polymer is remarkable. The formation of a linear polymer is also confirmed by the kinetic analysis of the laser-assisted reaction. The kinetic behavior is usually described by reporting the integrated area of a product band as a function of time (*2*, *5*). The integrated intensity of the infrared band due to the C=C stretching mode of the polymer is reported together with the best fit according to the Avrami law: $A_t/A_\infty = 1 - \exp[-k(t - t_0)^n]$, where $A_t$ is the integrated intensity at time $\pm$, $A_\infty$ is the same quantity measured when the reaction is concluded, $k$ is the rate constant, and $t_0$ is the time at which the reaction begins (*14*–*17*). The extremely good agreement with the Avrami model, even in the early stages of the reaction (nucleation step), is ascribed to the absence of a diffusion step involving the transport of the reactants to the reactive sites. The fit parameter $n$, which accounts for the polymer growth geometry, is equal to 1.86, therefore indicating a linear propagation of the reaction (*15*–*17*).

Butadiene is transparent at 488 nm, so it is most likely that irradiation at this wavelength induces a two-photon transition to the $2^1A_g$ excited state (*18*–*21*). This transition is symmetry allowed, and a high cross section has been calculated (*22*). The importance of the $2^1A_g$ state is central in the photophysics and photochemistry of polyenes (*23*–*25*). Most of the attention has been devoted to single molecule reactivity, leading either to cyclization or to

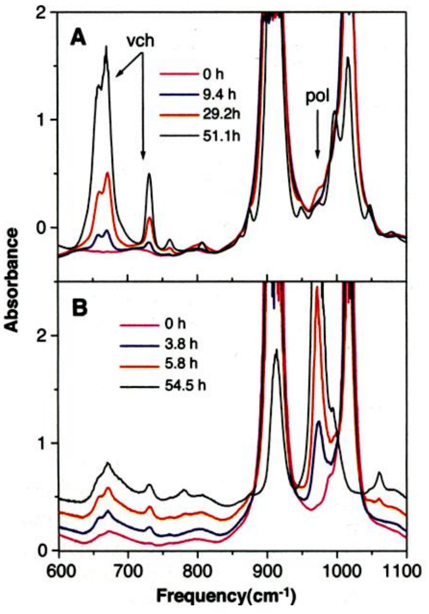

**Fig. 1.** IR spectra showing the kinetic evolution of the pressure-induced reaction in liquid butadiene at 0.8 GPa and 300 K (**A**) without laser irradiation and (**B**) while the sample was irradiated at 488 nm. Vch and pol refer to the characteristic absorption bands of vinylcyclohexene and of polybutadiene, respectively.

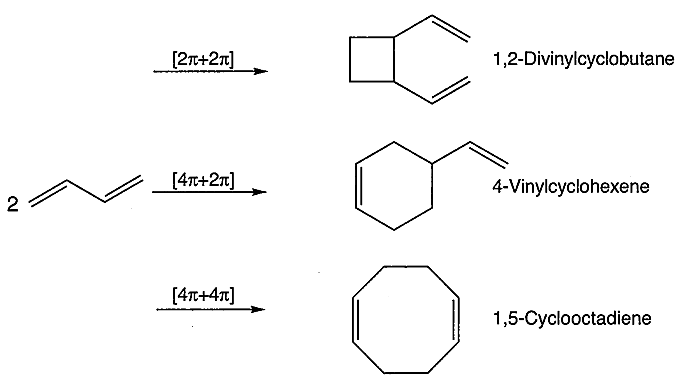

**Scheme 1.** Reaction paths for the dimerization of butadiene

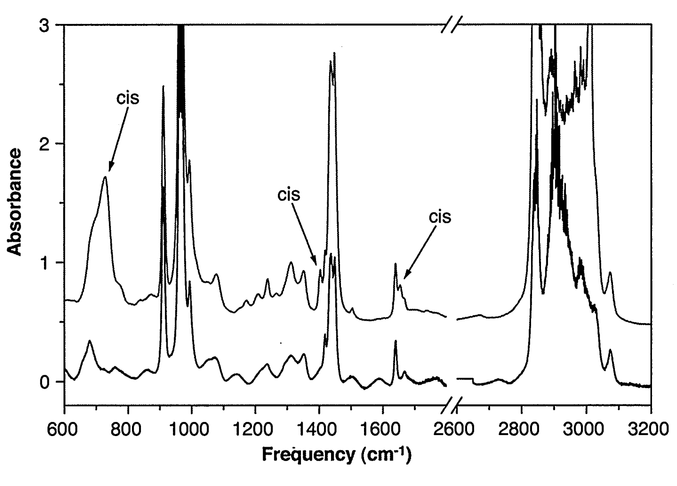

**Fig. 2.** Comparison between the IR spectra of the recovered compound of the laser-assisted reaction (lower trace) and commercial polybutadiene (upper trace) from Aldrich (composition 36% cis, 59% trans, and 5% 1,2 adduct).

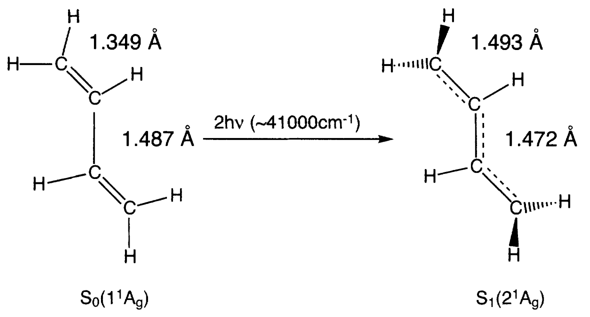

**Scheme 2.** Geometrical changes in the butadiene molecule induced by the $S_0 \rightarrow S_1$ two-photon electronic transition. The bond distances (*23, 24*) are expressed in Å.

cis-trans isomerization (*23, 24*), while experimental (*26*) and theoretical (*27*) studies on reactions involving more butadiene molecules are limited. These reactions seem to occur through conical intersections between the energy surfaces of the $S_1$ ($2^1A_g$) and the $S_0$ states (*24, 25, 27*), explaining the efficient nonradiative decay and the low selectivity (large number of products) of the photo-induced reactions.

The mechanism of the high-pressure polymerization can be pictured as follows. In the $S_1$ state, the outer $C_1$-$C_2$ and $C_3$-$C_4$ backbone bond lengths increase by ~10% compared with the ground state and become larger than the $C_2$-$C_3$ bond length (*28, 29*). This structural change is accompanied by a lowering of the torsional barrier such that a nearly free rotation of the terminal -$CH_2$ groups is possible (Scheme 2). The geometry changes, together with the long lifetime of the $S_1$ state, which allows collisions with the nearest neighbor molecules, favor a development of the reaction along the molecular backbone and, at the same time, prevent the dimerization, which requires an overlapping of π bonding electron densities of nearest neighbor molecules.

The present experiments give clear evidence that laser irradiation plays a fundamental role in the activation of the polymerization that prevails over the competing dimerization process. The obtainment of pure *trans*-polybutadiene is indeed a remarkable result. As a whole, the high-pressure reaction studied in the present report has several interesting features including the high selectivity of the process, the easy switching from one pathway to the other, and the full transformation into the product with the absence of solvents and catalysts, thus fulfilling several of the requirements for a green chemistry process (*30*).

### References and Notes

1. H. G. Drickamer, *Science* **156**, 3779 (1967).
2. C. S. Yoo, M. Nicol, *J. Phys. Chem.* **90**, 6732 (1986).
3. K. Aoki, Y. Kakudate, M. Yoshida, S. Usuba, S. Fujiwara, *J. Chem. Phys.* **91**, 778 (1989).
4. M. Sakashita, H. Yamawaki, K. Aoki, *J. Phys. Chem.* **100**, 9943 (1996).
5. M. Ceppatelli, M. Santoro, R. Bini, V. Schettino, *J. Chem. Phys.* **113**, 5991 (2000).
6. Ph. Pruzan, J. C. Chervin, M. M. Thiery, J. P. Itie, J. M. Besson, *J. Chem. Phys.* **92**, 6910 (1990).
7. F. Cansell, D. Fabre, J. P. Petitet, *J. Chem. Phys.* **99**, 7300 (1993).
8. L. Ciabini, M. Santoro, R. Bini, V. Schettino, *Phys. Rev. Lett.* **88**, 85505 (2002).
9. ——, *J. Chem. Phys.* **116**, 2928 (2002).
10. S. W. Benson, *J. Chem. Phys.* **46**, 4920 (1967).
11. G. H. Miller, *J. Polym. Sci.* **43**, 517 (1960).
12. A membrane DAC (MDAC), equipped with IIa-type diamonds, was used for the high-pressure IR absorption measurements. Butadiene (99.9% purity) was loaded in the MDAC by condensing the gas close to the melting point in an inert atmosphere. The initial sample dimensions were 50 μm thick and, depending on the experiment, 150 to 300 μm in diameter. Care was taken to maintain liquid butadiene to an initial pressure not exceeding 0.2 to 0.3 GPa. Pressure was measured by the ruby fluorescence method with the 514.5-nm emission of an $Ar^+$ laser as excitation line. The laser power was reduced to about 0.2 mW to avoid unintended laser effects on the reaction process. Infrared spectra were recorded, with an instrumental resolution of 1 $cm^{-1}$, with a Fourier transform IR (FTIR) (Bruker IFS-120HR) spectrometer. An optical condensing system was used to focus the IR beam on the small gasket hole (*31, 32*).
13. N. Neto, C. Di Lauro, *Eur. Polym. J.* **3**, 645 (1967).
14. See supplementary fig. 1 on *Science* Online at www.sciencemag.org/cgi/content/full/295/5562/2058/DC1.
15. M. Avrami, *J. Chem. Phys.* **7**, 1103 (1939).
16. ——, *J. Chem. Phys.* **8**, 212 (1940).
17. ——, *J. Chem. Phys.* **9**, 177 (1940).
18. There is some debate about the exact location of the $2^1A_g$ state. Calculations predicted the $2^1A_g$ state at 6 to 7 eV (*19*), but electron impact experiments by Doering *et al.* (*20*) locate the $1^1A_g \rightarrow 2^1A_g$ transition at 7.4 eV. The 488-nm $Ar^+$ line corresponds to a two-photon energy of 5.1 eV (~41,000 $cm^{-1}$) and is in much better agreement with the results of a resonance Raman investigation that locates the $2^1A_g$ state at about 44,300 $cm^{-1}$ (~5.5 eV) with a width of 4000 to 5000 $cm^{-1}$ (*21*). According to this latter estimate and considering the usual redshift of the excited electronic state at high pressure, irradiation in the present experiment corresponds to pumping in the low-frequency edge of the $2^1A_g$ level. Because in the present experiment the laser light is unambiguously absorbed via a two-photon mechanism, we are able to locate the $2^1A_g$ state of butadiene well below the calculated values in agreement with the results of resonance Raman spectroscopy (*21*).
19. K. B. Wiberg, C. M. Hadad, G. B. Ellison, J. B. Foresman, *J. Phys. Chem.* **97**, 13586 (1993), and references therein.
20. J. P. Doering, R. J. McDiarmid, *J. Chem. Phys.* **73**, 3617 (1980).
21. R. R. Chadwick, M. Z. Zgierski, B. S. Hudson, *J. Chem. Phys.* **95**, 7204 (1991).
22. V. Galasso, *J. Chem. Phys.* **89**, 4529 (1988).
23. B. E. Kohler, *Chem. Rev.* **93**, 41 (1993).
24. S. Zilberg, Y. Haas, *J. Phys. Chem. A* **103**, 2364 (1999).
25. M. Olivucci, I. N. Ragazos, F. Bernardi, M. A. Robb, *J. Am. Chem. Soc.* **115**, 3710 (1993).
26. I. Haller, R. Srinivasan, *J. Chem. Phys.* **40**, 1992 (1964).
27. M. J. Bearpark *et al.*, *J. Am. Chem. Soc.* **119**, 709 (1997).
28. M. Aoyagi, Y. Osamura, S. Iwata, *J. Chem. Phys.* **83**, 1140 (1985).
29. M. Aoyagi, Y. Osamura, *J. Am. Chem. Soc.* **111**, 470 (1989).
30. P. T. Anastas, T. C. Williamson, Eds., *Green Chemistry* (Oxford Univ. Press, Oxford, 1998).
31. R. Bini, R. Ballerini, G. Pratesi, H. J. Jodl, *Rev. Sci. Instrum.* **68**, 3154 (1997).
32. F. Gorelli, M. Santoro, L. Ulivi, R. Bini, *Phys. Rev. Lett.* **83**, 4093 (1999).
33. Supported by the European Union under contract HPRICT1999-00111 and by the Italian Consiglio Nazionale delle Ricerche and Ministero dell'Università e della Ricerca Scientifica e Tecnologica (MURST).

28 November 2001; accepted 8 February 2002

---

# Chromium Isotopes and the Fate of Hexavalent Chromium in the Environment

**Andre S. Ellis,[1] Thomas M. Johnson,[1]* Thomas D. Bullen[2]**

**Measurements of chromium (Cr) stable-isotope fractionation in laboratory experiments and natural waters show that lighter isotopes reacted preferentially during Cr(VI) reduction by magnetite and sediments. The $^{53}Cr/^{52}Cr$ ratio of the product was 3.4 ± 0.1 per mil less than that of the reactant. $^{53}Cr/^{52}Cr$ shifts in water samples indicate the extent of reduction, a critical process that renders toxic Cr(VI) in the environment immobile and less toxic.**

Chromium is a common contaminant in surface water and groundwater (*1, 2*) because it is used widely in electroplating and other industries and occurs naturally at high concentration in ultramafic rocks. Under oxidizing conditions, Cr is highly soluble and mobile as the Cr(VI) anions chromate ($CrO_4^{2-}$) and bichromate ($HCrO_4^-$). Cr(VI) is a suspected carcinogen (*3*). Under reducing conditions, Cr(VI) may convert to Cr(III), which is insoluble, strongly adsorbed onto solid surfaces (*4*), and less toxic. Cr(VI) can be removed from solution artificially by in situ reduction (*5, 6*), or naturally by reductants

---

[1] Department of Geology, University of Illinois at Urbana-Champaign, 245 Natural History Building, Urbana, IL 61801, USA. [2] Water Resources Division, U.S. Geological Survey, 345 Middlefield Road, Menlo Park, CA 94025, USA.

*To whom correspondence should be addressed. E-mail: tmjohnsn@uiuc.edu